Generalized surface, pseudosurface, and high-frequency pseudosurface acoustic waves on (001), (110), and (111) InSb

M. H. Kuok, S. C. Ng, and V. L. Zhang
Department of Physics, National University of Singapore, Singapore 119260, Republic of Singapore

S. J. Chua
Department of Electrical Engineering, National University of Singapore, Singapore 119260, Republic of Singapore

(Received 30 June 2000)

A comprehensive polarization Brillouin study has been carried out on the dependence of the phase velocities of the generalized surface, pseudosurface, and high-frequency pseudosurface acoustic waves on their propagation direction on the (001), (110), and (111) surfaces of InSb. The pseudosurface wave was found to have two angular dispersion branches arising from its respective sagittal and shear-horizontal displacement components. The dispersion curve of the latter was found to extend into regions which are not bounded by the two transverse bulk mode branches, where pseudosurface waves are conventionally thought to be absent. An observation of high-frequency pseudosurface modes in InSb is also reported.

I. INTRODUCTION

The absence of translational invariance, on the free surface of an anisotropic crystal, permits the existence of inhomogeneous acoustic modes consisting of bulklike and evanescent partial waves.[1,2] In particular, both an acoustic surface mode, the generalized surface wave (GSW), and two different types of radiating modes, called the pseudosurface wave (PSW) and the high-frequency pseudosurface wave (HFPSW) can exist. Of these only the GSW is a true surface mode. It possesses three partial waves, two of which propagate parallel to the surface, while the third decays exponentially within the crystal. Its Poynting vector is directed along the free surface. PSW has two of its three partial waves confined to the free surface while the third is a bulk wave propagating into the medium. Energy is radiated away from the surface and the mode suffers attenuation. PSW can propagate along certain specific directions on the surface of anisotropic crystals with the phase velocity lying between those of the fast and slow quasitransverse bulk modes (labeled by FTW and STW, respectively). With two of its three partial waves radiating energy into the bulk, HFPSW is more severely attenuated than PSW. HFPSW has a phase velocity slightly below that of the quasi-longitudinal bulk mode (LW) but above that of FTW propagating parallel to the surface. Because PSW and HFPSW radiate energy into the bulk, they are also referred to as leaky waves.

The phase velocities of GSW, PSW, and HFPSW in anisotropic crystals, are dependent on their propagation direction; the greater the anisotropy, the more marked the directional dependence. The anisotropic ratio $\eta[=2C_{44}(C_{11}-C_{12})^{-1}]$ gives a measure of the anisotropy in cubic crystals. With $\eta=1.99$, anisotropy in InSb is the most pronounced among the common semiconductors like Si ($\eta=1.57$), Ge ($\eta=1.67$), and GaAs ($\eta=1.80$).[3]

Brillouin scattering from surface acoustic waves in InSb has been studied by Aleksandrov *et al.*[4–6] using a five-pass Fabry-Perot interferometer. However, literature data on the surface acoustic waves in this semiconductor are far from complete. More importantly, computed power spectra of InSb reveal the existence of a pseudosurface mode with a shear-horizontal displacement component having a velocity which, contrary to conventional theory, does not lie between those of the two transverse bulk modes. Thus far, no experimental evidence of this predicted PSW feature has been reported for any anisotropic cubic crystal. Our work was motivated in part by the search for this component of PSW. Additionally, we intended to investigate the polarization behavior of GSW, PSW, and HFPSW on the (001), (110), and (111) surfaces of InSb over their entire dispersion ranges. We have measured, for instance, polarization spectra and the HFPSW on the (110) and (111) planes of InSb, results which have not been reported previously.

II. EXPERIMENT

Samples used were in the form of (001), (110), or (111)-oriented *n*-type InSb single-crystal wafers of resistivity $4\times10^{-2}\Omega$ cm. The polished wafers were oriented to a precision of $\pm0.5°$. Brillouin spectra were recorded using a JRS Scientific Instruments (3+3)-pass tandem Fabry-Perot interferometer, with a finesse of 120, used in conjunction with either an EG&G model SPCM-AQR-16 single-photon counting detector or a photomultiplier module rated at 0.9 dark counts/s. The free spectral ranges (FSR) were set between 10 and 25 GHz. All measurements were carried out in an air ambiance at room temperature. The 514.5-nm line of a Spectra Physics 2080-15S argon-ion laser was used, with beam power ranging from 100 to 125 mW incident on the samples. A stream of pure argon gas was directed at the irradiated spot on the samples to cool them and to keep air away. The experiment was performed in the 180° backscattering geometry using an $f/2.7$ collection lens. The horizontal incident light wave vector $\mathbf{k}$ made an angle of θ with either the [001], [110], or [111] surface normal and the backscattered light

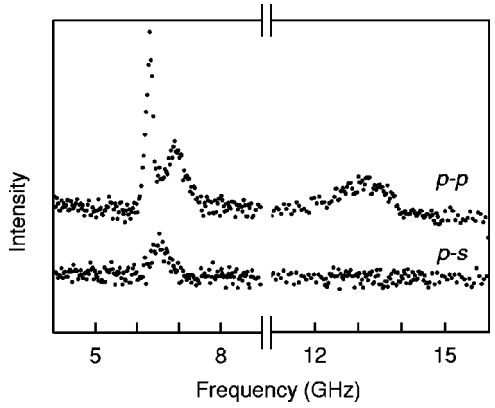

FIG. 1. Polarization Brillouin spectra of GSW, PSW, and HFPSW on the (110) surface of InSb recorded at $\phi=40°$ and $\theta=71°$.

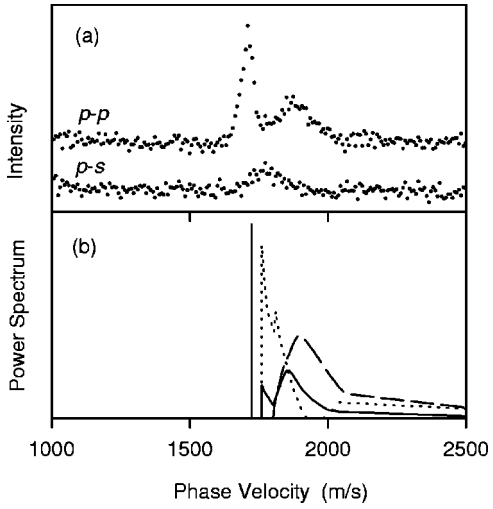

FIG. 2. (a) Polarization Brillouin spectra of GSW and PSW on (110) InSb recorded at $\phi=40°$ and $\theta=71°$. (b) Cartesian components of calculated power spectra of (110) InSb from Ref. 6. The longitudinal, shear-horizontal, and shear-vertical components are represented by solid, dotted, and dashed lines, respectively.

was collected from the solid angle around $-\mathbf{k}$, with the sagittal plane vertical.

Samples were mounted on a miniature two-axis translation stage attached to a rotation stage which permits variation in the azimuthal angle ϕ (the in-plane angle between the surface mode wave vector $\mathbf{q}$ and the reference crystal axis). The latter was, in turn, attached to a vertically mounted rotation stage, with their axes orthogonal, that allows variation in the incidence angle θ. The composite sample holder ensured that the same spot on the samples was irradiated at any angular setting of θ and ϕ. Brillouin spectra were recorded over entire angular periods, viz., ϕ ranges of 45°, 90°, and 30° for the (001), (110), and (111) planes, respectively. On these planes, ϕ is the angular displacement of the propagation direction of the surface wave from the respective [100], [001], and [110] crystal axes. All spectra were recorded in either the *p-p* or *p-s* scattering configuration with each spectral run varying from 1 to 4.5 h. Peaks appearing in the *p-p* configuration are due to shear-vertical (SV) surface excitations via the ripple scattering mechanism and to longitudinal ones via subsurface elasto-optic coupling. The *p-s* configuration contains peaks arising from shear-horizontal (SH) surface excitations via subsurface elasto-optic coupling.

III. RESULTS AND DISCUSSION

The recorded spectra are well polarized, as exemplified by Fig. 1 which shows two typical polarization spectra of the three surface acoustic modes on (110) InSb. The phase velocities V of the surface acoustic modes were calculated from their corresponding Brillouin frequencies ν, using

$$V=2\pi\nu/q. \tag{1}$$

The magnitude of the wave vector $\mathbf{q}$ of a surface mode is given by

$$q=4\pi\sin\theta/\lambda, \tag{2}$$

where λ denotes the incident light wavelength. Bulk mode phase velocities in InSb were determined using elastic stiffness constants[7] $C_{11}=67.2$, $C_{12}=36.7$, and $C_{44}=30.2$ GPa, as well as its density,[7] which was taken to be 5770 $\mathrm{kg\,m^{-3}}$.

Figure 1 shows *p-p* and *p-s* Brillouin spectra recorded at $\theta=71°$ and $\phi=40°$ for (110) InSb. The *p-p* spectrum contains three peaks at 6.3, 7.0, and 13.2 GHz with respective linewidths of 0.2, 0.6, and 1.8 GHz. Only one peak appears in the *p-s* spectrum. It has a frequency of 6.5 GHz and a linewidth of 0.5 GHz.

Aleksandrov *et al.*[6] have computed the power spectra for the various displacement components of surface modes propagating along certain directions on (110) InSb. Reference to Fig. 2 reveals that our results agree well with the power spectrum calculated for $\theta=70°$ and $\phi=40°$. Thus in the *p-p* polarization, the 6.3 GHz (1714 m/s) peak is attributed to GSW, while the 7.0 GHz (1905 m/s) peak is ascribed to the SV displacement component of PSW. The lone *p-s* polarized peak, at 6.5 GHz (1768 m/s), is identified as the SH displacement component of PSW, arising from the existence of SH excitation peaks in the continuum of surface states. The observation of the SH displacement component of PSW on this surface has, to our knowledge, not been reported before for any anisotropic cubic crystals, presumably because of its weak intensity and its proximity to the GSW mode and the other two PSW components. Lastly the *p-p* polarized peak at 13.2 GHz, in Fig. 1, as it has the highest energy and the widest linewidth, is assigned to HFPSW traveling on (110) InSb. Moreover, it is theoretically expected to have only a longitudinal displacement component.

Figures 3, 4, and 5 show the angular dispersion of the various surface modes propagating on the respective (110), (001), and (111) surfaces of InSb. Included in these figures are the calculated velocities of the two quasitransverse bulk modes (FTW and STW) and the longitudinal bulk mode (LW). The theoretical dispersion branches of GSW and the PSW sagittal displacement component are also reproduced in the dispersion diagrams.[3,6]

A. Generalized surface waves

In the dispersion diagrams (Figs. 3, 4, and 5), the bottommost dispersion curve is that of the GSW. For propagation

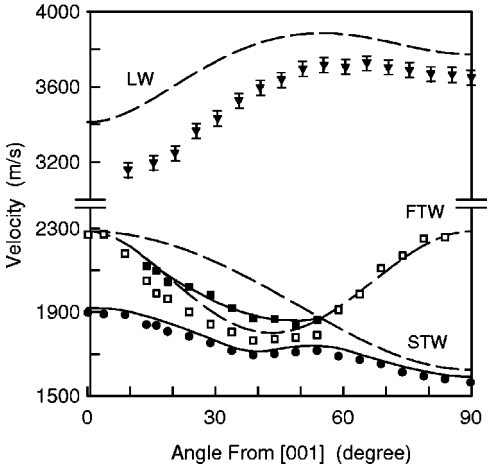

FIG. 3. Angular dispersion of surface acoustic modes on (110) InSb. The dashed lines represent the theoretical bulk mode branches, while the solid curves represent the calculated GSW and PSW branches. Experimental data for GSW, PSW (sagittal), and HFPSW are denoted by solid circles, squares, and inverted triangles, while those for PSW (SH) by open squares. The error bars for the GSW and PSW experimental data are smaller than the symbols used to represent them.

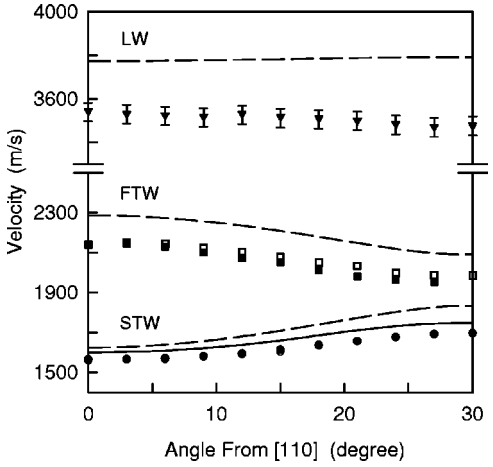

FIG. 5. Angular dispersion of surface acoustic modes on the (111) surface of InSb. The dashed curves represent the theoretical bulk mode branches while the solid curve represents the calculated GSW branch. Experimental data for GSW, PSW, and HFPSW are represented by circles, squares, and inverted triangles, respectively. Solid and open symbols denote the respective *p-p* and *p-s* polarization data. The error bars for the GSW and PSW experimental data are smaller than the symbols used to represent them.

on all the three basal planes, the measured curve, which extends over the full angular dispersion range, parallels the theoretical one,[8] with the measured velocities systematically 2% lower than the theoretical ones. Studies[5,9–12] have shown that surface wave velocities measured by Brillouin scattering (GHz range) are consistently lower than those determined by ultrasonic techniques (MHz range). Various explanations[9,10,13] have been advanced for this systematic discrepancy, but we will not concern ourselves with this.

For propagation on the (110) surface, GSW was observable in only *p-p* polarization for all propagation directions. However, on the (001) surface, GSW is a pure sagittal wave only along the [100] direction ($\phi=0°$). As the propagation direction is rotated away from the [100] direction, GSW gains a transverse horizontal displacement component. At $\phi=45°$, GSW degenerates completely into the slow quasitransverse bulk mode and as a consequence, it appears only in *p-s* polarization. For the (111) surface, while the sagittal component of GSW was detected over the entire angular dispersion range, its SH displacement component was observed only in the limited angular region of $0°\leqslant\phi\leqslant 18°$. However, the velocities of the two components are the same within experimental errors.

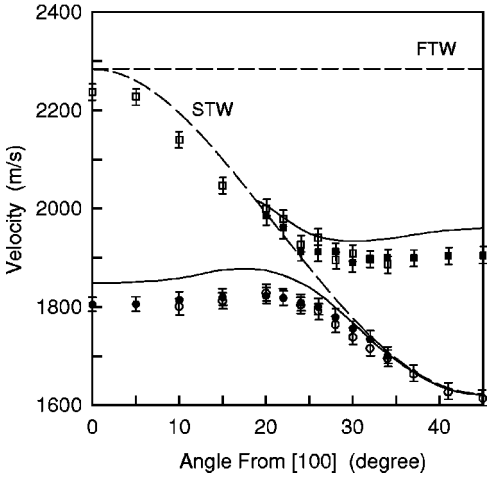

FIG. 4. Angular dispersion of surface acoustic modes on the (001) surface of InSb. The dashed lines represent the theoretical bulk mode branches, while the solid curves represent the calculated GSW and PSW branches. Experimental data for GSW and PSW are represented by circles and squares, respectively. Solid and open symbols denote the respective *p-p* and *p-s* polarization data.

B. Pseudosurface waves

The experimental angular dispersion curves of PSW follow well their theoretical ones. In general, our measured PSW velocities are some 2% consistently lower than the theoretical ones calculated using elastic constants determined by ultrasonic methods. This discrepancy is outside the experimental accuracy of 1%.

1. (110) surface

Theoretical calculations by Farnell[3] show that no pseudosurface mode is expected on the (110) surface of all cubic crystals with an anisotropic ratio greater than one. Contrary to his prediction, experimental evidence of its existence, on this surface, has been reported.[4–6] Indeed we discovered that it is observable for all propagation directions on the (110) surface of InSb.

For $\phi<55°$ ($\phi\approx 55°$ corresponds to propagation along the [111] direction; it also corresponds with the intersection of the two transverse bulk mode branches), there exist two experimental branches of PSW, associated with its respective sagittal and SH displacement components (see Fig. 3). The former mirrors the theoretical curve calculated by taking the maxima of the SV displacement component of the power spectra.[6] The SV branch of PSW is bounded by the two quasitransverse bulk mode curves. It is noteworthy that the

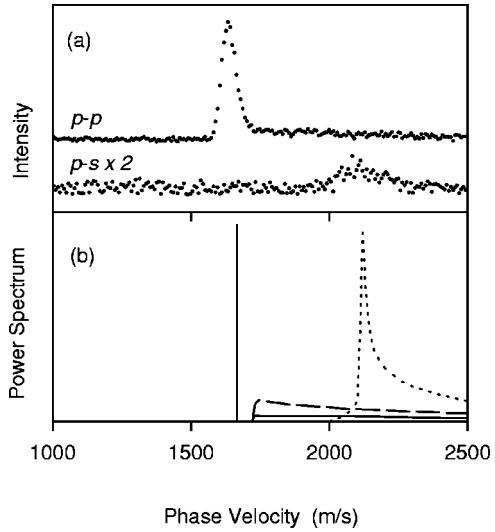

FIG. 6. (a) Polarization Brillouin spectra of GSW and PSW on (110) InSb recorded at $\phi=70°$ and $\theta=71°$. (b) Cartesian components of calculated power spectra of (110) InSb from Ref. 6. The longitudinal, shear-horizontal, and shear-vertical components are represented by solid, dotted, and dashed lines, respectively.

SH branch, which has been predicted (from the presence of SH peaks in computed power spectra, as discussed above) but not previously observed, lies below the STW curve. This is unusual as PSW velocities are conventionally thought to lie between those of the two transverse bulk modes. The PSW degenerates into the quasitransverse bulk modes along the [111] direction. Interestingly, for $\phi>55°$, a region theoretically devoid of PSW, a peak is still observed in the *p-s* Brillouin spectrum. Figure 6 shows that the *p-s* polarized Brillouin peak, at 2120 m/s, coincides with the calculated intense threshold excitations, of SH character, in the $\phi=70°$ power spectrum.[6] Based on this, the peak is assigned to the SH displacement component of PSW. It is noted that the SH branch of PSW follows well the FTW curve.

The angular variation of the Brillouin linewidth of the *p-p* polarized PSW on the (110) surface of InSb is shown in Fig. 7. It agrees qualitatively with the predicted attenuation of this mode in (110) GaAs, computed from the imaginary part of its velocity.[6] Interestingly the region of high attenuation

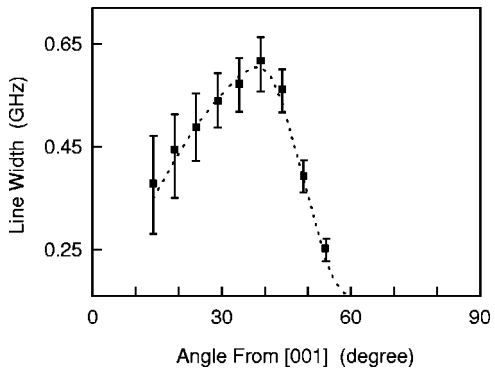

FIG. 7. Angular dependence of the experimental linewidth of the sagittal displacement component of PSW on (110) InSb. The dotted curve is only a guide for the eye.

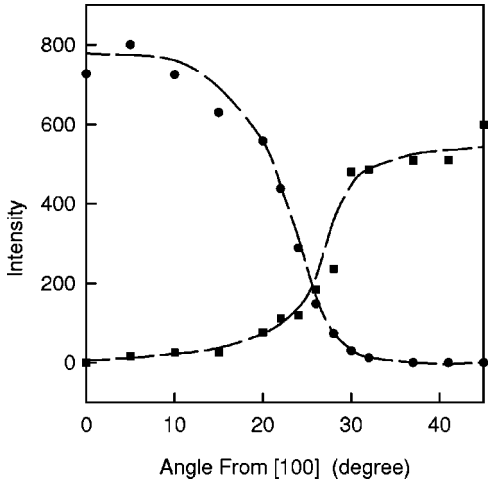

FIG. 8. The angular variation of the Brillouin intensities of GSW (denoted by circles) and PSW (denoted by squares) for *p-p* scattering from (001) InSb. The errors are smaller than the size of the symbols. The dashed curves are only a guide for the eye.

corresponds to the angular range over which *p-p* polarized PSW was observed. Scattering from this component of PSW is more intense than that from its *p-s* polarized component.

2. (001) surface

Our preliminary results[14] show that on the (001) surface, PSW can propagate along only certain directions with velocities lying between those of the two transverse bulk modes, corresponding to the angular region, $20°\leqslant\phi\leqslant 45°$. This observation is consistent with theory. At $\phi=45°$ (the [110] direction), the PSW is a Rayleigh-type wave having purely sagittal polarization. As ϕ decreases, it develops a transverse displacement component normal to the sagittal plane at the expense of the sagittal components until, at $\phi\approx 20°$, it degenerates into the STW. It is noteworthy that from $\phi\approx 20°$ down to 0°, a weak peak, with a velocity comparable to that of PSW, still appears in the *p-s* Brillouin spectrum. Within this range of ϕ, the velocity of this Brillouin peak does not lie between those of FTW and STW (see Fig. 4). Hence no PSW is expected in this angular region. However, as discussed above, a similar case was discovered for the propagation of the SH displacement component of PSW on the (110) plane. Based on this, the *p-s* polarized Brillouin peak is also attributed to the SH displacement component of PSW.

Another notable feature is that the measured angular dispersion of GSW and PSW, on (001) InSb, traces out two separate and distinct branches, in accordance with theory (see Fig. 4). This contrasts sharply with the measured crossover, at an azimuthal angle $\phi\approx 30°$, of the GSW to PSW reported for anisotropic cubic crystals[5,9–11,13,15–17] including InSb.[18]

The angular variation of the Brillouin intensities of GSW and PSW for *p-p* scattering, displayed in Fig. 8, is consistent with the angular dependence of their scattering cross sections computed by Stoddart *et al.*[13] for (001) Si. For instance, the GSW intensity is maximal for propagation along the [100] direction ($\phi=0°$), decreasing gradually until at $\phi\approx 20°$ it drops sharply. At $\phi\approx 30°$ it becomes very weak, finally

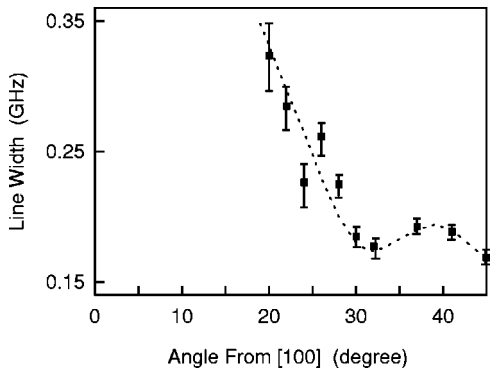

FIG. 9. Angular dependence of the experimental linewidth of the sagittal displacement component of PSW on (001) InSb. The dotted curve is only a guide for the eye.

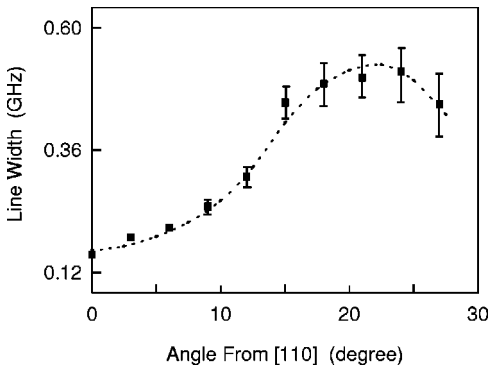

FIG. 10. Angular dependence of the experimental linewidth of the sagittal displacement component of PSW on (111) InSb. The dotted curve is only a guide for the eye.

becoming barely visible at $\phi = 45°$ at which point it degenerates into a transverse bulk mode. The angular variation of the pseudosurface mode intensity is opposite to that of the GSW. At $\phi \approx 26°$, the two surface modes appear with equal intensity in *p-p* scattering, in accordance with theory.

The experimental linewidth of the *p-p* polarized PSW is plotted as a function of its propagation direction in Fig. 9. The angular variation of the linewidth correlates reasonably well with the predicted angular variation of the calculated attenuation of this mode on (001) InSb.[5] In particular our results lend support to the existence of a predicted minimum in the linewidth at about $\phi = 32°$.

3. (111) surface

The *p-p* scattering from PSW, on the (111) InSb surface, is most intense at the azimuthal angle $\phi = 0°$ ([110] direction), becoming weaker with increasing ϕ and is not detectable in the neighborhood of $\phi = 30°$ (see Fig. 5). A similar behavior has been observed for PSW traveling on the (111) surface of Si by Kuok *et al.*[12] These observations are consistent with the theoretical findings of Lim and Farnell.[8] They predicted that as ϕ approaches 30°, the penetration depth of PSW into the bulk increases, until at $\phi = 30°$, at which point it degenerates into a transverse bulk wave which, because of its SH character, does not contribute to *p-p* scattering.

The PSW peak, in contrast, always appears in the *p-s* Brillouin spectrum for all propagation directions on the (111) surface. This peak is narrowest at $\phi = 0°$, and progressively broadens as the wave vector **q** of PSW is rotated away from the [110] direction. This behavior is consistent with the power spectra of surface displacement components on the (111) surface of GaAs calculated by Carlotti *et al.*[1]

The linewidth of PSW in the *p-p* polarized Brillouin spectrum as a function of its propagation direction is shown in Fig. 10. The angular variation of the linewidth is qualitatively consistent with the angular variation of the attenuation calculated for the pseudosurface mode on (111) GaAs by Carlotti *et al.*[1] In particular, both the experimental linewidth and the theoretical attenuation peak at about $\phi = 20°$.

C. High-frequency pseudosurface waves

The existence of HFPSW in InSb was observed by Brillouin spectroscopy. However, of the three basal planes examined, the presence of HFPSW could only be detected on the (110) and (111) surfaces. This is not surprising as HFPSW is rarely observed on the (001) surface. The topmost row of data points, in Figs. 3 and 5, represents the measured angular dispersion of HFPSW on these two respective planes. This high-frequency leaky mode, with a velocity slightly below that of LW but above that of FTW, is present in only *p-p* scattering, thus confirming its theoretically predicted pure sagittal character.[1]

On the (110) surface, the HFPSW intensity is greatest for propagation directions in the angular region around the [110] direction and gets progressively weaker with decreasing ϕ until it vanishes for ϕ below $\approx 10°$. In contrast, Fig. 5 shows that the velocity of this mode is not particularly sensitive to changes in its propagation direction on the (111) surface. The HFPSW has a sagittal character and its intensity increases with increasing azimuthal angle ϕ from 0° to 30°.

IV. CONCLUSION

We have measured the *p-p* and *p-s* polarization Brillouin spectra of GSW, PSW, and HFPSW on the (001), (110), and (111) surfaces of InSb as a function of their propagation direction over the entire range of angular dispersion. Shear-horizontal displacement components of PSW, on (001) and (110) surfaces, with phase velocity below that of STW, have been detected. The polarization character of the three surface acoustic modes was found to be consistent with theoretical predictions. The angular dependence of the Brillouin linewidths of the pseudosurface mode agrees qualitatively with the computed angular dispersion of its attenuation. Additionally, HFPSW have been observed on the (110) and (111) surfaces of InSb.

ACKNOWLEDGMENTS

This work was supported by the National University of Singapore under research project No. R-144-000-018-112 and through the award of financial support to V. L. Zhang.

[1] G. Carlotti, D. Fioretto, L. Giovannini, F. Nizzoli, G. Socino, and L. Verdini, J. Phys.: Condens. Matter **4**, 257 (1992).
[2] R.E. Camley and F. Nizzoli, J. Phys. C **18**, 4795 (1985).
[3] G.W. Farnell, *Physical Acoustics*, edited by W.P. Manson and R.N. Thurston (Academic Press, New York, 1970), Vol. VI, p. 109.
[4] V.V. Aleksandrov and J.B. Potapova, Solid State Commun. **84**, 401 (1992).
[5] V.V. Aleksandrov, T.S. Velichkina, J.B. Potapova, and I.A. Yakovlev, Phys. Lett. A **171**, 103 (1992).
[6] V.V. Aleksandrov, A. Gladkevitch, V.G. Mozhaev, L. Giovannini, and F. Nizzoli, J. Appl. Phys. **76**, 2176 (1994).
[7] *Surface Wave Velocities*, edited by A.J. Slobodnik, Jr., E.D. Conway, and R.T. Delmonico, Microwave Acoustics Handbook Vol. 1A (Air Force Cambridge Research Laboratories, Hanscom AFB, MA, 1973).
[8] T.C. Lim and G.W. Farnell, J. Acoust. Soc. Am. **45**, 845 (1969).
[9] J.R. Sandercock, Solid State Commun. **26**, 547 (1978).
[10] M. Mendik, S. Sathish, A. Kulik, G. Gremaud, and P. Wachter, J. Appl. Phys. **71**, 2830 (1992).
[11] P.R. Stoddart, J.D. Comins, and A.G. Every, Phys. Rev. B **51**, 17 574 (1995).
[12] M.H. Kuok, S.C. Ng, Z.L. Rang, and T. Liu, Solid State Commun. **110**, 185 (1999).
[13] P.R. Stoddart, J.C. Crowhurst, A.G. Every, and J.D. Comins, J. Opt. Soc. Am. A **15**, 2481 (1998).
[14] M.H. Kuok, S.C. Ng, and V.L. Zhang, Appl. Phys. Lett. **77**, 1298 (2000).
[15] J.O. Kim and J.D. Achenbach, Thin Solid Films **214**, 25 (1992).
[16] D.W. Schindel, D.A. Hutchins, S.T. Smith, and B. Farahbakhsh, J. Acoust. Soc. Am. **95**, 2517 (1994).
[17] V.R. Velasco and F. Garcia-Moliner, Solid State Commun. **33**, 1 (1980).
[18] V.V. Aleksandrov, T.S. Velichkina, V.G. Mozhaev, and I.A. Yakovlev, Solid State Commun. **77**, 559 (1991).